International Journal of Heat and Mass Transfer 54 (2011) 1527–1537

Contents lists available at ScienceDirect

International Journal of Heat and Mass Transfer

journal homepage: www.elsevier.com/locate/ijhmt

Numerical simulation of convective heat transfer between air flow and ceramic foams to optimise volumetric solar air receiver performances

Zhiyong Wu [a,b], Cyril Caliot [b], Gilles Flamant [b], Zhifeng Wang [a,*]

[a] The Key Laboratory of Solar Thermal Energy and Photovoltaic System, IEE-CAS, Beijing 100190, China
[b] Processes, Materials, and Solar Energy Laboratory, PROMES CNRS, 7 Rue du Four Solaire, 66120 Font-Romeu, France

ARTICLE INFO

Article history:
Received 1 December 2009
Received in revised form 15 July 2010
Accepted 13 October 2010

Keywords:
Porous media
Tetrakaidecahedral model
Local volumetric heat transfer coefficient
Nusselt number correlation
Volumetric solar air receiver
Computational fluid dynamics

ABSTRACT

Porous ceramic foams are used to achieve high performance in solar heat recovery systems. Understanding the convective heat transfer between the air flow and the ceramic foam is of great importance when optimising the volumetric air receiver. In this work, the convective heat transfer was numerically studied. The present approach was designed to compute the local convective heat transfer coefficient between the air flow and a porous ceramic foam. For that purpose, the energy balance and the flow inside the porous ceramic foam were solved. In addition, a detailed geometry of the porous ceramic foam was considered. The ceramic foams were represented by idealised packed tetrakaidecahedron structures. The numerical simulations were based on the three dimensional Reynolds-averaged Navier–Stokes (RANS) equations. A sensitivity study on the heat transfer coefficient was conducted with the porosity, velocity and mean cell size as parameters. Based on the numerical simulation results, a correlation for the volumetric local convective heat transfer coefficient between air and ceramic foams was developed. The resulting correlation covers a wide range of porosities, velocities, cell sizes and temperatures. The correlation results were compared with experimental data from the literature, and the comparison shows good agreement. The correlation is intended to be used in the design of volumetric solar air receivers.

1. Introduction

Because foam materials have unique structural properties, such as large surface area and low density, they are now being widely used in various industries, for example, as catalyst supports in chemistry, heat exchangers in electrical cooling, low emission combustors in energy and volumetric air receivers in concentrated solar power [1–3]. The heat exchange between the solid matrix and the fluid flowing through it is encountered in most of these applications. The heat transfer between the surface of the struts and the fluid is of great importance because it couples the temperature field between the fluid and solid phases [4]. Fuller [5] mentioned that there are two different mechanisms by which the foam structure enhances the heat transfer. The first mechanism is linked to the foam structure, which causes the flow to be more turbulent, thus increasing the heat transfer. This is sometimes referred to as "thermal dispersion". The second is the extended surface offered by the foam, which consequently enhances the exchanged heat. In concentrated solar power applications, ceramic foams are usually used as solar radiation absorbers that transfer the absorbed energy to a flowing fluid. The knowledge of heat transfer characteristics between the solid framework and the carrier fluid is thus crucial for the successful design and steady operation of a volumetric solar air receiver.

The micro-structure of ceramic foams is highly irregular, and no obvious representative cell structure exists in a bulk ceramic foam samples. The strut surface is irregular, the flow path inside the bulk material is tortuous, and thus only the volume averaged flow fields (temperature, velocity and pressure) exhibit regular behaviour. Consequently, it is difficult to choose the suitable characteristic length for the study of flow and heat transfer in ceramic foams [6,7]. It is also difficult to quantify the convective heat transfer between the solid surface and the fluid either by experiment or numerical simulation. Many researchers have ignored the heat transfer between the fluid phase and the solid phase by assuming that the two phases are in local thermal equilibrium (LTE) [8,9]. In opposition to the LTE model, the local thermal non-equilibrium (LTNE) model assumes that there is a finite temperature difference between the fluid and the porous phase. The LTNE model uses two energy equations to describe the heat transfer within the bulk porous media. The two coupled partial differential equations account for the energy conservation of the fluid and solid phases, respectively. Many theoretical and numerical studies [10–14] have used the thermal non-equilibrium model. Specifically, Coussirat et al. [15] and Guardo et al. [16] investigated the particle-to-fluid heat transfer by numerical simulation. However, most of them have

* Corresponding author. Tel.: +86 10 62520684; fax: +86 10 62587946.
E-mail address: zhifeng@vip.sina.com (Z. Wang).

0017-9310/$ - see front matter © 2010 Elsevier Ltd. All rights reserved.
doi:10.1016/j.ijheatmasstransfer.2010.11.037

Nomenclature

a_v	specific surface area ($m^2\ m^{-3}$)
d	mean cell diameter (m)
d_p	mean pore diameter (m)
d_s	mean strut radius (m)
h	mean wall heat transfer coefficient ($W\ m^{-2}\ K^{-1}$)
h_l	local wall volumetric heat transfer coefficient ($W\ m^{-2}\ K^{-1}$)
h_{lv}	local volumetric heat transfer coefficient ($W\ m^{-3}\ K^{-1}$)
h_v	mean volumetric heat transfer coefficient ($W\ m^{-3}\ K^{-1}$)
L	thickness of the sample (m)
L_c	critical length (m)
L_e	entrance length (m)
L_s	strut length (m)
Nu	Nusselt number based on h
Nu_l	Nusselt number based on h_l
Nu_v	Nusselt number based on h_v
Nu_{lv}	Nusselt number based on h_{lv}
Pr	Prandtl number $\mu/(\rho\lambda)$
q_v	volumetric heat flow ($W\ m^{-3}$)
Q	heat flux ($W\ m^{-2}$)
Q_l	local heat flux ($W\ m^{-2}$)
Re	Reynolds number ($\rho ud/\mu$)
T	temperatures (K)
u	superficial velocity ($m\ s^{-1}$)
u_p	mean pore velocity ($m\ s^{-1}$)
z	z-directional coordinate (m)

Greek symbols

λ	thermal conductivity ($W\ m^{-1}\ K^{-1}$)
τ	tortuosity
ε	porosity
ρ	fluid density ($kg\ m^{-3}$)
μ	dynamic viscosity ($kg\ m^{-1}\ s^{-1}$)
v	kinematic viscosity ($m^2\ s^{-1}$)

Subscripts

s	solid
f	fluid
l	Local
p	pore
v	volume
in	inlet
out	outlet

used simple geometries, such as a periodic array of square cylinders [17], square rods [18] and a cubic model [19]. Petrasch et al. [20,21] obtained the real geometry of reticulate porous ceramics by using computed tomography (CT) and then studied the penetrability and interfacial heat transfer characteristics of this porous material by numerical simulation. Petrasch's methodology is better than the works based on idealised geometry because his geometry is closer to the real micro-structure of the reticulate porous ceramics. However, Petrasch and co-workers' methodology needs sophisticated characterisation and long computational effort.

There are two reported techniques for measuring the heat transfer coefficient of a foam-filled channel: a steady state method [5,22] and a transient (single-blow) method [6,23–25]. The heat transfer coefficient measured through the steady state method is inherently dependent on the thermal conductivity of the foams because of the heat source located at the side surface of the channel, and it is usually used for comparison with an empty channel. The transient method is widely used to obtain the convective heat transfer coefficient between the strut surface and the flow stream. The convective heat transfer coefficient from the single-blow method is assumed to be independent on the thermal properties of the solid phase. The results from both methods are global and lead to averaged coefficients. Because of the complexity of the internal morphology of the porous medium, it is extremely difficult to experimentally study the flow and the heat transfer at the pore scale geometry. So far, most of the experimental studies of heat transfer in foam materials are confined to bulk samples. To put it simply, the detailed heat transfer information inside a bulk foam sample cannot be acquired by experiments.

It is rather difficult to measure the geometrical parameters of foam materials such as the specific surface area, mean cell size and mean pore size. Consequently, a new parameter, the "volumetric heat transfer coefficient, h_v", was defined and adopted by many researchers [6,25,26] to describe the heat exchange performance of foam materials. This coefficient reflects the average heat transfer characteristics over a porous matrix volume. In the literature [6,25–28], several correlations have been reported for the relationship between the volumetric heat transfer coefficient and the Reynolds number. The general form of these correlations is $Nu_v = C_1 Re^{m_1} Pr^{n_1}$. Wu et al. [29] investigated the convective heat transfer characteristics of air flow through ceramic foams numerically, and argued that it is not appropriate to use the "mean volumetric heat transfer coefficient" and proposed to use the local volumetric heat transfer coefficient to evaluate the heat exchange performance of foam materials. The reason is that the wall heat transfer coefficient is not constant inside the entire porous matrix, and above all, there often exists a thermal equilibrium region. The mean volumetric heat transfer coefficient overlooks these phenomena and smoothes the temperature discrepancy between the fluid and the solid phase.

For engineering applications of porous media, solving the volume-averaged LTNE model is the most convenient solution. The difficulty in using this model is knowing the convective heat transfer coefficient between the fluid and the solid phase and also the relationships between the interfacial heat transfer coefficient and the geometrical properties of the porous medium. The aim of this study was to investigate the heat transfer characteristics between the flowing fluid and strut surface of ceramic foams. For that purpose, the flow and the energy balance were solved in an idealised geometry with standard CFD tools. The ceramic foam geometry was represented by periodic regular structures formed with packed tetrakaidecahedra. Based on the numerical results, a correlation of the local volumetric heat transfer coefficient as a function of cell size, porosity and velocity was developed. This paper is a contribution toward understanding the convective heat transfer in porous media and may help in the design of volumetric solar air receivers.

2. Geometry, control equation and numerical method

2.1. Geometry

Ceramic foams can be described as a reticulated structure of open cells with typically 12–14 pentagonal or hexagonal faces [30]. However, many idealised regular geometry models, for example, the cubic model (Dul'nev model) [31,32], the face-centred model, the body-centred model [33], Weaire–Phelan's unit cell

[34] and Kelvin's tetrakaidecahedral model [35,36], were used to numerically study the pressure drop, convective heat transfer and radiation heat transfer in foams. In theory, Weaire–Phelan's model is better able to represent the fine structure of foam materials compared to Kelvin's model. However, the difference between Weaire–Phelan's model and Kelvin's model is very small, and Weaire–Phelan's model is more difficult to build. Among all the existing models, the tetrakaidecahedral model is by far the most widely used model. In this study, a periodical structure formed by packed tetrakaidecahedra was used to represent the real ceramic matrix (see Fig. 1). The following relationships (simplified formulas were used to calculate the volume of the solid phase), which were directly deduced through the tetrakaidecahedron model, have been used in this study.

$$d = 2.828L_s \tag{1}$$

$$\varepsilon = 1 - \frac{9.425}{8\sqrt{2}}\left(\frac{d_s}{L_s}\right)^2 + \frac{3.33}{8\sqrt{2}}\left(\frac{d_s}{L_s}\right)^3 \tag{2}$$

In addition, the foam morphological structure shows that the surface of the struts transitions smoothly at the junction, and thus the face-blend structure was used at the junction of struts (see Fig. 2). By adding the face-blend structure and adjusting the curvature of the blend faces and the mean diameter of the struts, the real porosity of the tetrakaidecahedral model can be adjusted. In this study, the curvature radius of the blend face was 0.1–0.3L_s, depending on the porosity.

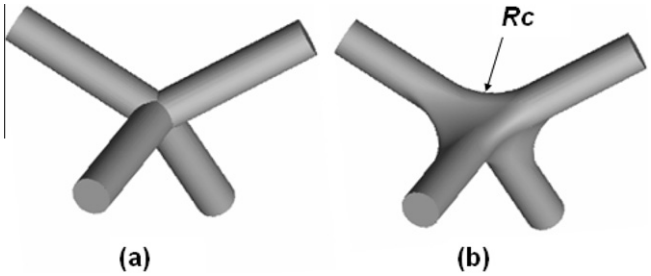

Fig. 2. The face-blend structure. (a) Strut junction without treatment. (b) Strut junction with face-blend treatment (curvature radius *Rc* is adjustable).

2.2. Governing equations

The governing equations are based on the three dimensional steady Reynolds-averaged Navier–Stokes equations, which consist of the conservation equations of mass, momentum and energy [37]. In this study, the superficial velocity ranged from 0.5 m/s to 6 m/s, the relative static pressure (with reference pressure 101,325 Pa) ranged from 200 Pa to 3000 Pa, and the temperature ranged from room temperature to 1225 K. Thus, variable properties of the air were used in this study. The laws of the air properties changing with temperature are described in [38].

The air was treated as an ideal gas when computing the density. The effects of the gravity force were neglected in the momentum equations. The radiative heat transfer inside the bulk ceramic foams was not taken into account because the air can be treated as a non-participating medium, and the solid was at uniform temperature.

2.3. Numerical method

2.3.1. Grid generation

The flow paths inside of the ceramic foams are highly tortuous (see Fig. 1); thus, the flow regimes in the pores continuously impinge and separate. In the ceramic foams, the turbulence intensity is very high: it can reach 0.6–0.8 [39]. Both impinging, separation and recirculation flows are very difficult to predict in numerical simulation. They require a very fine grid for accurately simulation of the intense turbulent flow. The grids consisted of tetrahedral elements, and five layers of prism grids were used as the boundary layer grid near the strut walls where large velocity and temperature gradients usually exist. The criterion used to set the first nodes near the wall was $y^+ < 2$ (y^+ is a non-dimensional wall distance). A grid independence study was conducted by checking the pressure

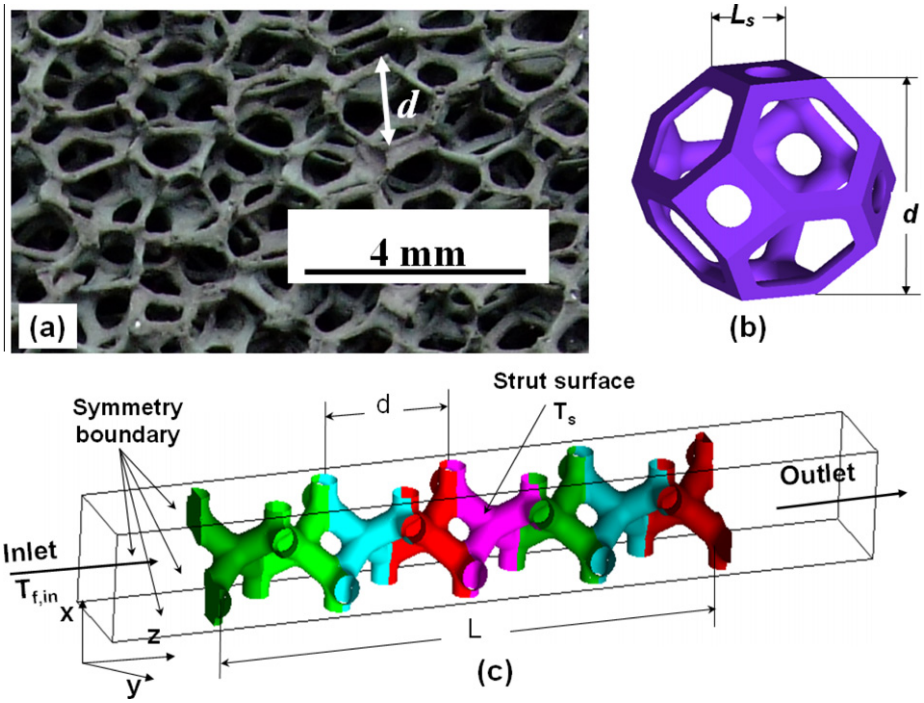

Fig. 1. Geometry used in this study. (a) Photo of ceramic foams, (b) unit tetrakaidecahedron cell, (c) computational domain and boundary conditions.

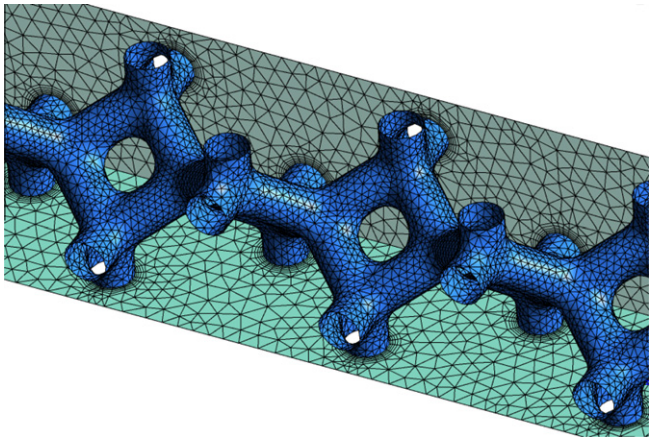

Fig. 3. Grid used in this study (boundary layer and surface mesh).

drop and the integrated heat flux with three sets of grid. The results showed that a grid with about 800,000 elements is fine enough, and a finer grid does not improve the results of the simulation. The final grid used in this paper was approximately 800,000 elements (see Fig. 3).

2.3.2. Turbulence model

To choose the turbulence model, it first should be clarified whether or not the flow regime is turbulent. The widely used criterion for distinguishing different flow regimes is the Reynolds number; unfortunately, there are many ways to calculate the Reynolds number for flow in a foam material. Wu et al. [7] summarised the methods for choosing the characteristic length of porous media and concluded that although there are many methods in the literature to define the characteristic length, these methods are essentially the same and the calculated Reynolds number values are very close. In this study, the mean cell size was used as the characteristic length.

The Reynolds number, which is based on the mean cell size and the superficial velocity ($Re = \rho u d/\mu$), ranges from 120 to 800 in this study. According to Kaviany [4], the flow regime is unsteady and chaotic. Wilcox [40] presented an overview of most of the modern turbulence models and stated that today's models yield accurate predictions for either wall-bounded flows or free-shear flows, but not both. Recently, Vieser and Menter [41,42] concluded that the SST model in combination with an optimal wall treatment provides highly accurate results for a wide variety of heat transfer cases. In this study, the SST k–ω model was chosen for all the computing cases. Note that the Re number in [4] is based on the pore diameter and average pore velocity, instead of the mean cell size and superficial velocity. The corresponding Reynolds numbers based on Kaviany's definition ranges from 240 to 1600. Strictly speaking, a part of the flow regime is laminar flow. However, a preliminary numerical study shows that the difference between the laminar flow and the turbulence model is insignificant. Thus, we always choose the SST k–ω model in this study.

2.3.3. Boundary condition

A velocity-inlet boundary condition with a uniform value was defined at the entrance of the inlet channel, and the static temperature was 300 K. A pressure-outlet boundary condition with zero gauge pressure (relative pressure, with reference pressure 101,325 Pa) was employed at the outlet boundary. All of the strut surfaces were defined as non-slip, non-penetrating walls with a constant temperature of 330 K for the parametric study and 700 K and 1200 K for validating the proposed model at high temperature. In addition, it was assumed that the macro-flow was one-dimensional and that the averaged streamline was parallel to the four side surfaces of the computational domain; thus, the four side surfaces were defined as symmetrical boundary conditions.

2.3.4. Numerical method

The three-dimensional RANS equations were solved using the commercial CFD software FLUENT. The double precision, coupled algorithm was used to couple the pressure and velocities. The second-order upwind advection model was used in the momentum, turbulent kinetic energy and turbulent energy dissipation equations. In the present calculations, the convergence criterion was set to 10^{-5}.

3. Results and discussion

3.1. Discussion about the flow field characteristics

Wu et al. [7] studied the flow field of air flow through ceramic foams under low temperature (less than 350 K) by numerical simulation and concluded that the entrance length (defined according to the velocity field) L_e is about 1–2 mean cell size long for Reynolds numbers less than 400. The trend is that L_e increases with Reynolds number, and the border effects only exist at the windward side. In addition, the static pressure linearly decreases along the flow direction, and the mean velocity accelerates at the entrance side and fluctuates heavily (constant when averaging the velocity over a volume that is larger than the representative element volume) inside the porous medium.

In this study, the fluid properties were defined as variable; thus, the momentum equations were coupled with the energy equation. Fig. 4 shows the mean static pressure distribution along the flow direction. It illustrates that the static pressure has a linear relationship with the distance. However, if the temperature range in the computational domain is large, there is little deviation of the linear relationship in the windward side. This is because a large temperature gradient exists in this region, which causes considerable change in the viscosity and density of the air. Fig. 5 shows the mean velocity distribution along the flow direction. It illustrates that the fluid accelerates in the region of thermal non-equilibrium because the density of air decreases with temperature. In addition, there is also large velocity fluctuation inside the bulk porous medium, which is very helpful for enhancing the convective heat transfer between the flowing fluid and strut surfaces.

Fig. 6 gives the distribution of the dimensionless temperature differences along the flow direction. Where the dimensionless temperature difference was defined as $(T_s - T_f)/(T_s - T_{f,in})$. It shows that the fluid temperature exponentially increases along the flow direction, and the exponent decreases with the Reynolds number. The distance from the porous border to the thermal equilibrium point is very short, about 10 times the mean cell size.

3.2. Convective heat transfer parameters in the porous medium

Conventionally, there are two ways to define the convective wall heat transfer coefficient, i.e., the *mean* or *local* wall convective heat transfer coefficient. For the convective heat transfer in foam materials, the *mean* or *local* volumetric convective heat transfer coefficients are also used. These heat transfer coefficients are defined as

$$h = \frac{Q}{A(T_s - T_f)} \tag{3}$$

$$h_l = \frac{Q_l}{A_l(T_{ls} - T_{lf})} \tag{4}$$

$$h_v = \frac{Q}{V(T_{ls} - T_f)} = h a_v \tag{5}$$

$$h_{lv} = \frac{Q_l}{V_l(T_{ls} - T_{lf})} = h_l a_v \tag{6}$$

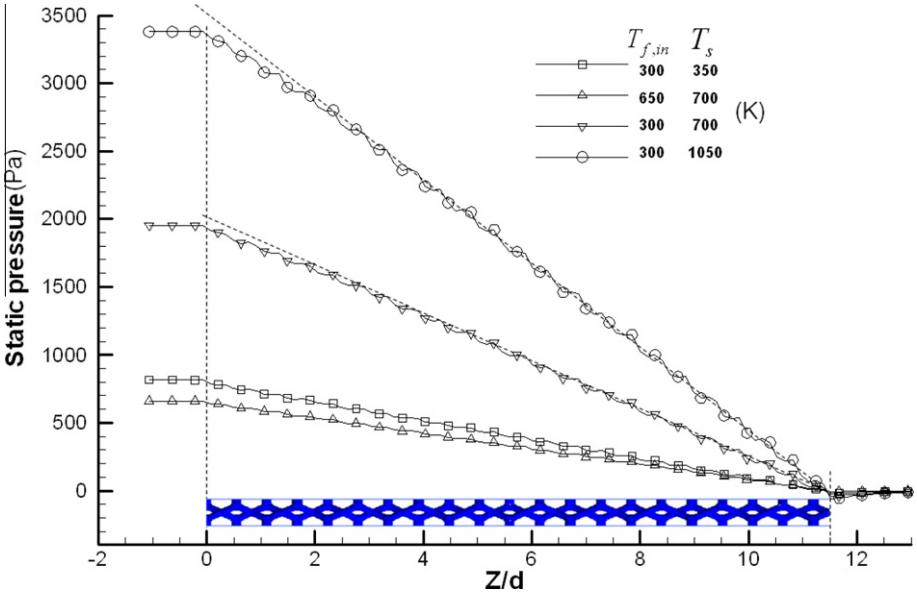

Fig. 4. The static pressure distribution along the flow direction (u = 5 m/s).

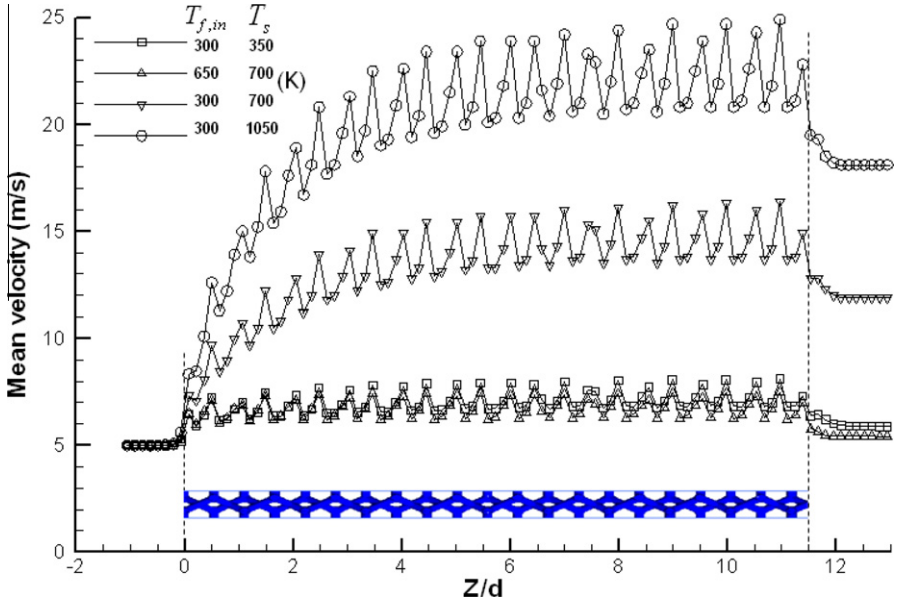

Fig. 5. The mean velocity distribution along the flow direction (u = 5 m/s).

The corresponding Nusselt numbers are defined as

$$Nu = \frac{hd}{\lambda} \tag{7}$$

$$Nu_l = \frac{h_l d}{\lambda_l} \tag{8}$$

$$Nu_v = \frac{h_v d^2}{\lambda} = Nu a_v d \tag{9}$$

$$Nu_{lv} = \frac{h_{lv} d^2}{\lambda_l} = Nu_l a_v d \tag{10}$$

In Eqs. (3)–(10), Q is the heat flux, A is the surface area, T is the mean temperature, V is the volume of foam material, λ is the thermal conductivity, and a_v is the specific surface area. The subscript l indicates a local parameter, the subscript s indicates the solid phase, and f indicates the fluid phase. See Fig 2, A means the overall strut surface area, and A_l, which means the local strut surface area and are in different colours. In this study, it is very important to note that the local parameter was considered at a pore-level average and also that the wall temperature was defined as constant; thus, $T_{ls} = T_s = constant$.

The local wall and local volumetric heat transfer coefficient are used in this work to study the comparative effects of the two main physical parameters in these cases. Another reason to use the local wall and local volumetric heat transfer coefficient is for future use in the LTNE model.

3.3. Local heat transfer coefficient

3.3.1. The characteristics of the local heat transfer coefficient and its influencing factors

In the grid generating stage, the strut surface mesh was divided into many parts (see Fig. 1c where different parts are in different colours). The size of neighbouring parts is equal to half of the mean cell size. For each part, the integrated surface area was defined as the local surface area A_l, and the integrated heat flux was defined as local heat flux Q_l. The mass-weighted average temperature of

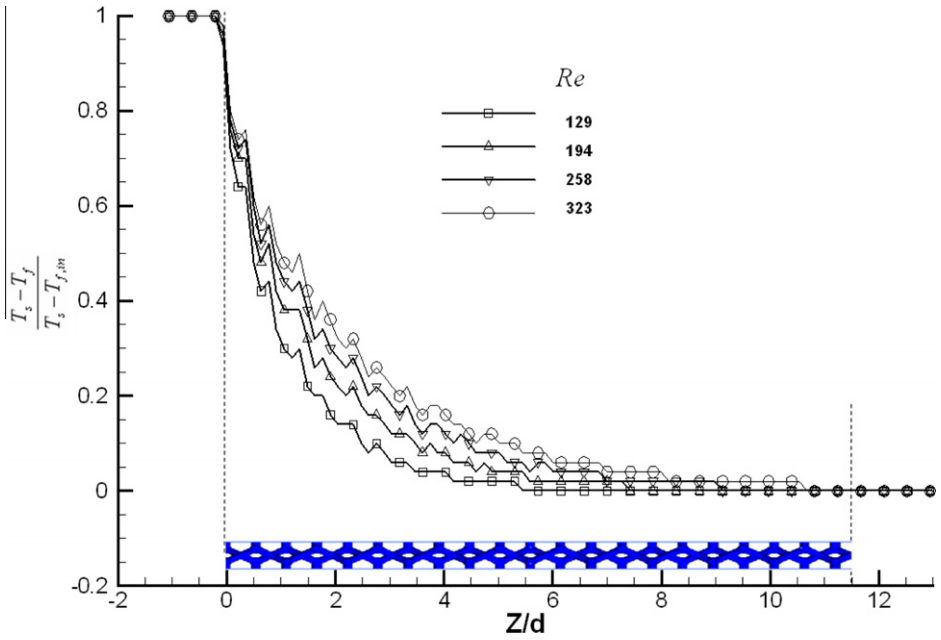

Fig. 6. The temperature distribution along the flow direction.

a plane, which is perpendicular to the flow direction and in the middle of each part, was used as the fluid temperature T_{lf}. The wall temperature was always T_s because it was defined as constant in this study. In this way, the local wall and volumetric heat transfer coefficient on the strut surface can be respectively calculated according to Eqs. (4) and (6).

Fig. 7 plots the local wall heat transfer coefficient distribution along the flow direction. This result illustrates that the local wall heat transfer coefficient on the strut surfaces is generally far larger than convective heat transfer on a smooth plane or in a pipe and is comparable with the heat transfer coefficient of an impinging flow. There are three reasons for this phenomenon. The first is that the pore structure causing the flow regime is inherently similar to a jet flow when the air leaves the pores and is similar to an impinging flow when the air reaches the struts. The second is that the tortuous flow paths cause the flow to become more turbulent, thus increasing the mixing of flows of different directions. The third reason is that the velocity is very large compared with the other cases, especially because the air density decreases with the temperature so that the air accelerates in the convective heat transfer region.

Fig. 7 also shows that the local wall heat transfer coefficient is high near the windward border region, then it decreases for a short distance and reaches a minimum, and finally it slowly increases before reaching a plateau. This distribution along the flow direction

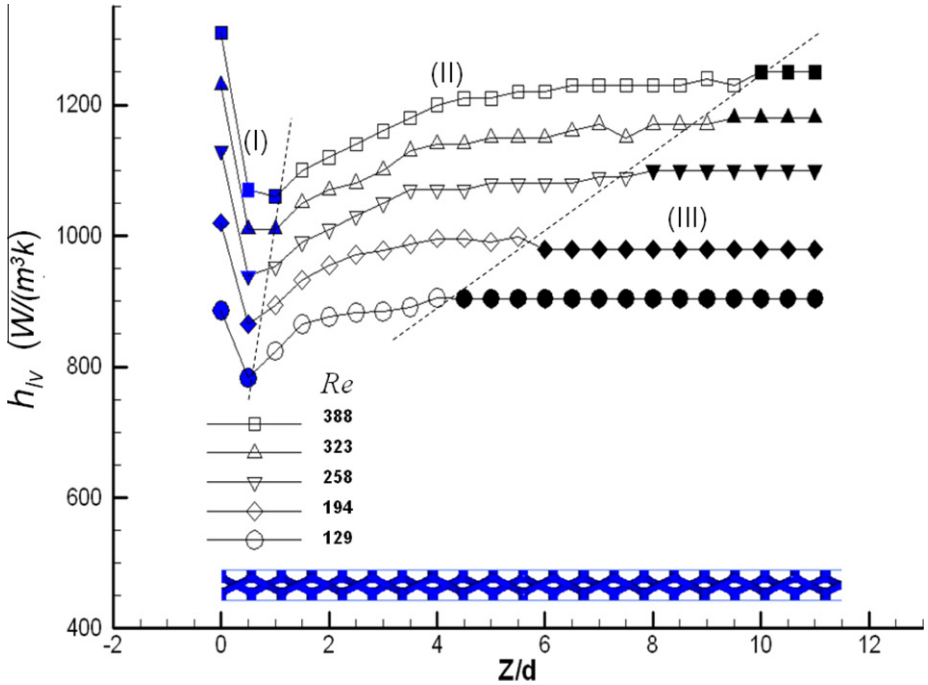

Fig. 7. The local wall heat transfer coefficient distribution along the flow direction: (I) boundary affected region, (II) stable convective region, (III) thermal equilibrium region.

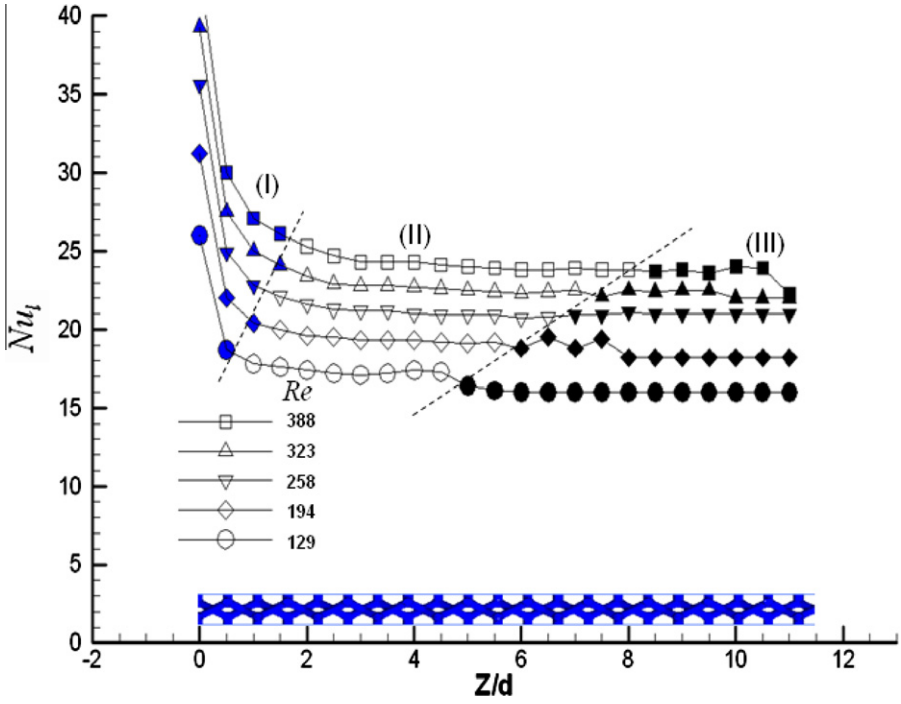

Fig. 8. The local Nusselt number distribution along the flow direction: (I) boundary affected region, (II) stable convective region, (III) thermal equilibrium region.

can be classified into three parts, each governed by one of three distinctive heat transfer mechanisms. The three regions are the boundary affected region, the stable convective region and the thermal equilibrium region. The heat transfer coefficient in the boundary affected region is very large because the air accelerates at the windward side of the porous matrix and directly impinges the strut surface. In the stable convective region, the wall heat transfer coefficient weakly increases. This is because the thermal conductivity and the velocity increase with temperature. Fig. 8 plots the local Nusselt number vs. the thickness z/d, which illustrates that the Nusselt number is approximately constant in the stable convective region even if the air properties vary. In this stable convective region and in the thermal equilibrium region, the flow is fully developed. In the thermal equilibrium region, the fluid temperature is equal to the solid temperature; thus, there is no heat transfer between the fluid and the solid. In theory, the local wall heat transfer coefficient should remain constant.

Figs. 9–11 present the relationship between the local wall heat transfer coefficient and the mean pore diameter, superficial velocity and porosity. The computed results show that the local wall heat transfer coefficient is strongly dependent on the mean pore diameter and superficial velocity and weakly dependent on

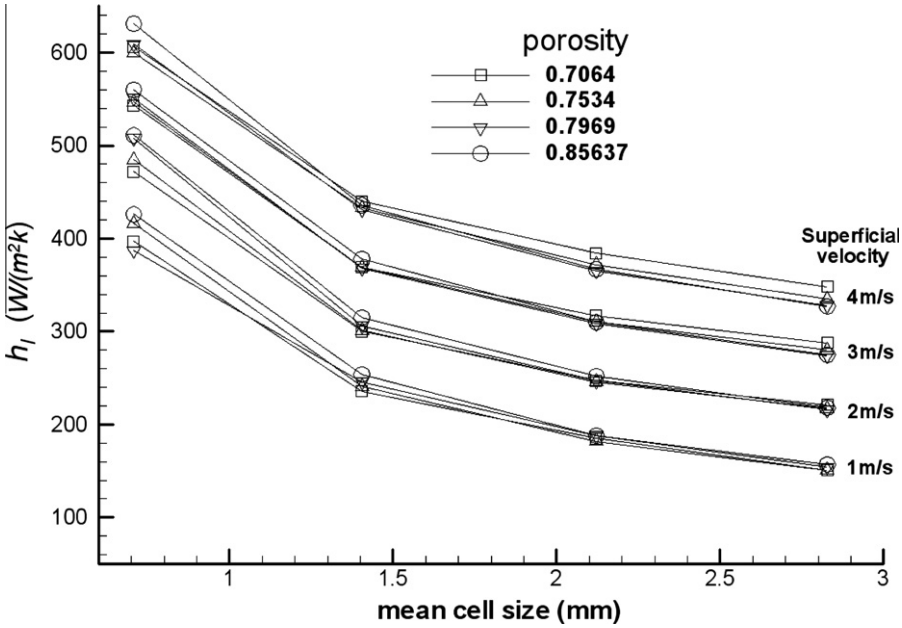

Fig. 9. The relationship between local wall heat transfer coefficient and mean cell size.

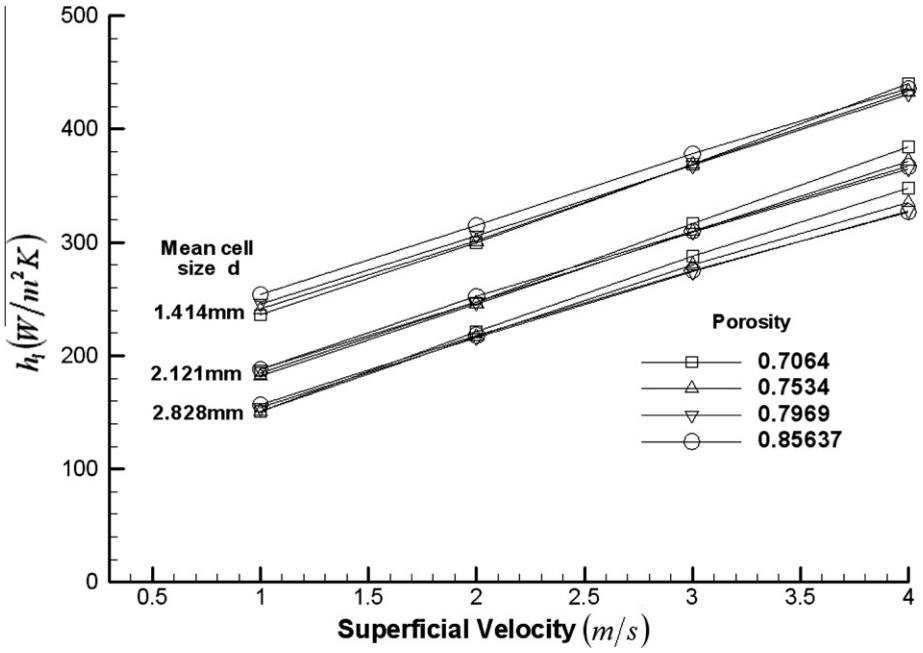

Fig. 10. The relationship between local wall heat transfer coefficient and velocity.

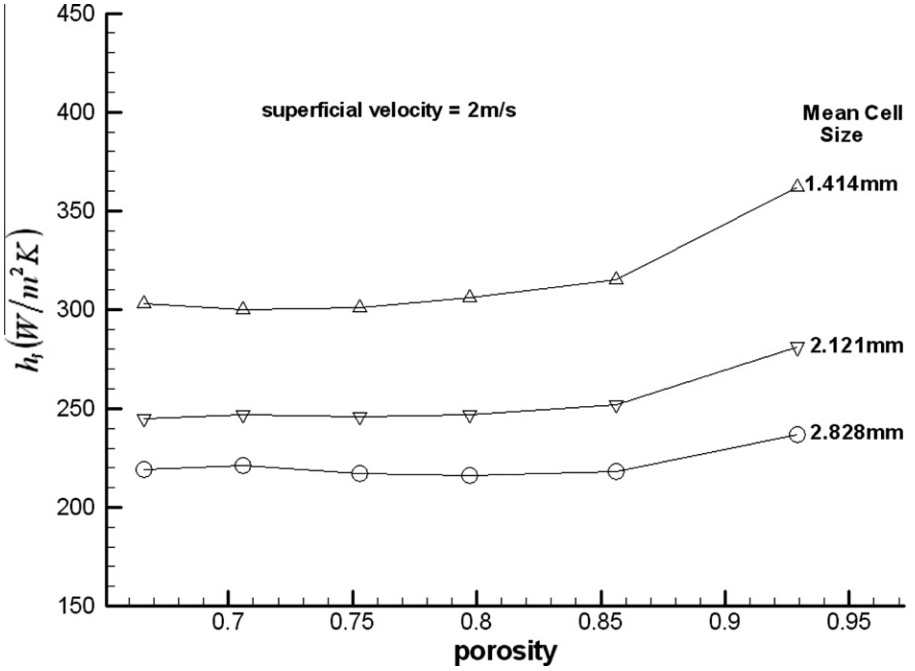

Fig. 11. The relationship between local wall heat transfer coefficient and porosity.

porosity in the ranges of the parameter variations studied. The local wall heat transfer coefficient decreases rapidly when the mean cell size increases, because the characteristic length decreases. It is obvious that the local wall heat transfer coefficient increases with the superficial velocity. The local wall heat transfer coefficient is weakly dependent on the porosity because the structural changes are not prominent when the porosity is in the range of 0.66–0.93. From these figures, we can see that the relationships are non-linear between the wall heat transfer coefficient and the superficial velocity, mean cell size and porosity.

3.3.2. Generalised correlation

For the case of single-fluid flows in porous media, the heat transfer is the same as that in a pipe, in a channel or on a flat plate. The main differences are the shape of the surfaces that participate in the heat transfer and the flow phenomenon in the pores. In the pores, the flow field is so stochastic and irregular that the volume average methodology is viewed as the best solution.

Now we start from some basic heat transfer correlations. For the fully developed turbulent flow in a pipe, Dittus–Boelter [43]

proposed $Nu = 0.023Re^{0.8}Pr^{n}$. For the tube bank in cross flow, Zhukauskas and Ulinskas [44] proposed $Nu = CRe^{m}Pr^{0.36}(Pr/Pr_s)^{1/4}$. For a packed bed, Wakao and Kaguei [45] found that the correlation for the convective heat transfer can be represented by $Nu = 2.0 + 1.1Re^{0.6}Pr^{1/3}$. (In the above correlations, the Reynolds number is based on the average velocity.) In addition, for the convective heat transfer in foam materials, some correlations from experimental studies in the literature [6,25,28] have the form of $Nu_v = CRe^{m}$ (here, the Reynolds number is based on the superficial velocity; for porous media, the average velocity is sometimes termed the mean pore velocity). All of the above mentioned correlations have similar forms and the empirical parameters rely on different geometries. Thus, we conclude that for the convective heat transfer between the air flow and the strut surface of ceramic foams, the dimensionless Nusselt number has the form of: $Nu_v = cRe^{m}$ (here, the Pr of the air was treated as a constant and merged with the coefficient c because it changes little with the temperature and the pressure). This form of correlation is also suitable for the local Nusselt number Nu_{lv}. Figs. 9–11 illustrate the non-linear relationships between the local wall heat transfer coefficient and mean cell size d, superficial velocity u and porosity ε. Thus, we assume the correlation for the Nusselt number has the form of: $Nu_{lv} = c\varepsilon^{m_1}Re^{m_2}$. This assumption is made for taking into account the effect of the porosity, and above all, the resulting expression for the correlation is dimensionally homogeneous.

For the study of porous media, the superficial velocity u is widely used, instead of the averaged pore velocity u_p. According to the mass conservation theory, the projection of u_p in the flow direction, i.e., $u_{p,axial}$, is equal to u/ε. The relationship between the mean pore velocity and its projection in the flow direction is $u_p = \tau u_{p,axial}$, where τ is the tortuosity of the average flow path in a porous medium. Thus, the relationship between the mean pore velocity and superficial velocity is

$$u_p = \frac{\tau u}{\varepsilon} \tag{11}$$

However, information regarding tortuosity is scarce. There are several tortuosity–porosity relations in the literature [46–49]. In [49], Shen and Chen showed that these correlations match each other well for porosities larger than 0.4 ($\varepsilon \geqslant 0.4$). For values of porosity ε near 1 (the porosity of the ceramic foams used in volumetric air receivers is about 0.8–0.9), the tortuosity in ceramic foams can be approximated as

$$\tau = \frac{1}{\varepsilon} \tag{12}$$

Thus, the relationship between the mean pore velocity and superficial velocity is

$$u_p = \frac{u}{\varepsilon^2} \tag{13}$$

In the present study, the superficial velocity was used in the definition of the Reynolds number, and thus the equation for the local wall heat transfer coefficient becomes

$$Nu_l = \frac{h_l d}{\lambda_l} = c\varepsilon^{m2}Re^{m1} \tag{14}$$

From the parametric studies on the mean cell size d, the superficial velocity u and the porosity ε, different values of h_l were obtained from the simulations. The simulations were conducted with air flow through ceramic foams under the porosity in the range of $0.66 < \varepsilon < 0.93$ and a Reynolds number between $70 < Re < 800$. In addition, the values of the heat transfer coefficient were taken inside the fully developed flow region, where it is constant if the air properties can be treated as constant values (when the temperature range in the computational domain is small). After fitting, the following correlation was obtained

$$Nu_l = 2.0696\varepsilon^{0.38}Re^{0.438} \tag{15}$$

The fitting error was less than 5%. This showed that the assumption of the form for the correlation is right, and the fitting work was successful.

In order to derive the volumetric heat transfer coefficient, we used Eq. (6). The specific surface area, a_v, is given in Wu et al. [7]. With the expression of the local Nusselt number given in Eq. (10), the previous correlation becomes

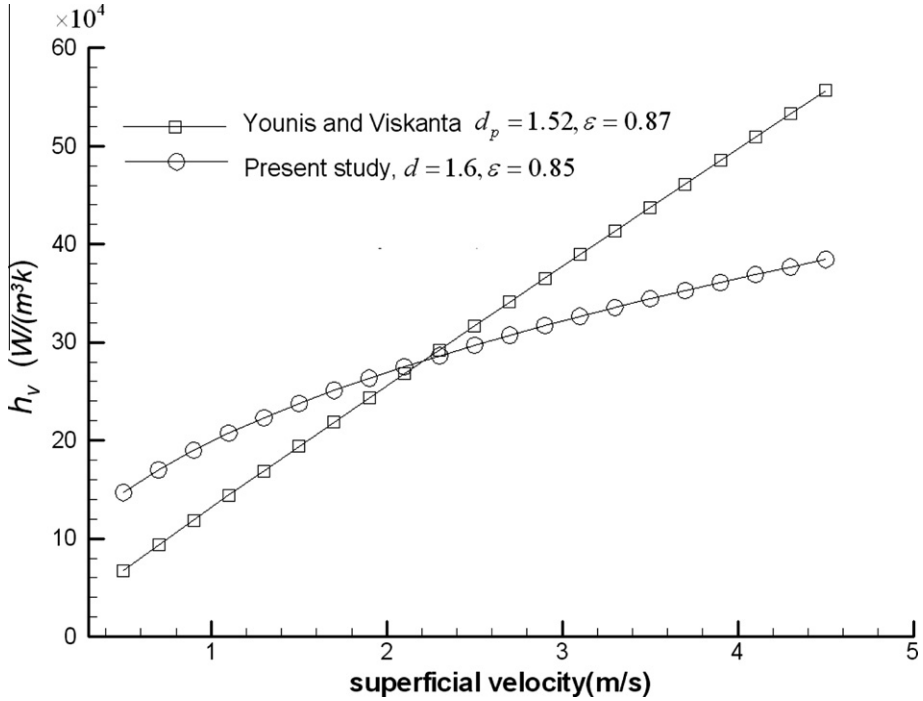

Fig. 12. Comparison between the correlation (25) and the experimental data.

$$Nu_{lv} = \frac{h_{lv} d^2}{\lambda_l} = 2.0696\varepsilon^{0.38} a_v Re^{0.438} = (32.504\varepsilon^{0.38} - 109.94\varepsilon^{1.38} + 166.65\varepsilon^{2.38} + 86.98\varepsilon^{3.38}) Re^{0.438} \quad (16)$$

This correlation is valid for porosity in the range of $0.66 < \varepsilon < 0.93$ and a Reynolds number in the range $70 < Re < 800$.

The typical value of the convective heat transfer coefficient of air flowing in a tube or a plate is 30–300 ($W\,m^{-2}\,K^{-1}$) [50]. In this study, the computed wall heat transfer coefficient is in the range of 100–600 ($W\,m^{-2}\,K^{-1}$) (see Figs. 9–11), which is higher than the typical values. This increment is due to the high turbulence intensity in porous medium, and thus we can conclude that the numerical results in this study are in agreement with reality.

When treating the air properties as constant and ignoring the border effect, the local volumetric heat transfer coefficient should be equal to the mean volumetric heat transfer coefficient and therefore comparable. Fig. 12 presents a comparison of the volumetric heat transfer coefficient (if the temperature is less than 350 K, then the air properties can be treated as constant) predicted by correlation (16) and models from the literature [25]. Compared with the experimental data from Younis and Viskanta [25], the predictive value agrees well at a superficial velocity of 2.2 m/s, is larger when $u < 2.2$ m/s and is smaller when $u > 2.2$ m/s. In the range of $1 < u < 4.5$ m/s, the predicted value of h_v is with 40% deviation from Younis's correlation. Overall, we can say the predictive value is on the same order as the experimental data from Younis and Viskanta [25]. In addition, the trend of the relationship between the volumetric heat transfer coefficient with mean cell size is consistent with Younis's study.

Moreover, there are geometrical discrepancies between the idealised packed tetrakaidecahedra and the real porous ceramic foam. The real porous matrix is comprised of cells with different diameters, all of the struts surfaces are rough instead of smooth, and there are always manufacturing flaws in the real foam material. Thus, further experimental study is needed to validate the correlations (15) and (16) and their accuracy.

4. Conclusions

This work numerically simulates the convective heat transfer in ceramic foams represented by an idealised packed tetrakaidecahedra structure. The model used to solve the air flow in the ceramic foam was presented. The inlet air temperature was kept smaller than the constant temperature of the ceramic foam to study the convective heat transfer coefficient values. Parametric studies were performed with different mean pore diameters, porosities, temperatures and velocities. The flow field and heat transfer characteristics were analysed in detail. The results are summarised below:

(1) The static pressure linearly decreases along the flow direction. Even in a large temperature range, the linear relationship can still be used. The mean velocity increases in the entrance zone and continues to increase in the thermal non-equilibrium region, then remains constant. The velocity field presents large velocity fluctuations throughout the entire porous medium. The mean fluid temperature exponentially changes along the flow direction, and as the Reynolds number increases, the exponent decreases.

(2) The calculated local (wall and volumetric) heat transfer coefficients versus the medium depth vary as follows: they are high in the entrance region, exhibit a minimum and then weakly increase in the thermal non-equilibrium region. The local (wall and volumetric) heat transfer coefficient increases with the Reynolds number and decreases with the mean cell size, and it is weakly dependent on the porosity. In addition, the local Nusselt number is constant in the fully developed region.

(3) Generalised correlations of the local wall/volumetric heat transfer coefficient in ceramic foams have been proposed for the first time. These correlations are useful for any design work related to ceramic foam applications.

Acknowledgment

This project was financially supported by the National Basic Research Program of China (2010CB227106).

References

[1] M. Becker et al., Theoretical and numerical investigation of flow stability in porous materials applied as volumetric solar receivers, Solar Energy 80 (10) (2006) 1241–1248.
[2] T. Fend et al., Two novel high-porosity materials as volumetric receivers for concentrated solar radiation, Solar Energy Mater. Solar Cells 84 (1–4) (2004) 291–304.
[3] T. Fend et al., Porous materials as open volumetric solar receivers: experimental determination of thermophysical and heat transfer properties, Energy 29 (5–6) (2004) 823–833.
[4] M. Kaviany, Principles of Heat Transfer in Porous Media, Springer, 1995.
[5] A.J. Fuller et al., Measurement and interpretation of the heat transfer coefficients of metal foams, Proc. Inst. Mech. Eng. C J. Mech. Eng. Sci. 219 (2) (2005) 183–191.
[6] X. Fu, R. Viskanta, J.P. Gore, Measurement and correlation of volumetric heat transfer coefficients of cellular ceramics, Exp. Thermal Fluid Sci. 17 (4) (1998) 285–293.
[7] Z. Wu et al., Experimental and numerical study on pressure drop in ceramic foams for volumetric solar receiver applications, Apllied Energy 87 (2) (2010) 504–513.
[8] S.A. Khashan, M.A. Al-Nimr, Validation of the local thermal equilibrium assumption in forced convection of non-Newtonian fluids through porous channels, Transport Porous Media 61 (3) (2005) 291–305.
[9] P.X. Jiang, Z.P. Ren, B.X. Wang, Numerical simulation of forced convection heat transfer in porous plate channels using thermal equilibrium or non-thermal equilibrium models, Numer. Heat Transfer 35 (Part A) (1999) 99–113.
[10] I.A. Badruddin et al., Numerical analysis of convection conduction and radiation using a non-equilibrium model in a square porous cavity, Int. J. Thermal Sci. 46 (1) (2007) 20–29.
[11] P.X. Jiang, Z.P. Ren, Numerical investigation of forced convection heat transfer in porous media using a thermal non-equilibrium model, Int. J. Heat Fluid Flow 22 (1) (2001) 102–110.
[12] S.A. Khashan, A.M. Al-Amiri, I. Pop, Numerical simulation of natural convection heat transfer in a porous cavity heated from below using a non-Darcian and thermal non-equilibrium model, Int. J. Heat Mass Transfer 49 (5–6) (2006) 1039–1049.
[13] A.M. Hayes et al., The thermal modeling of a matrix heat exchanger using a porous medium and the thermal non-equilibrium model, Int. J. Thermal Sci. 47 (10) (2007) 1306–1315.
[14] A.M. Hayes, The Thermal Modeling of a Matrix Heat Exchanger Using Porous Media and the Thermal Non-equilibrium, University of South Carolina, 2006.
[15] M. Coussirat et al., Performance of stress-transport models in the prediction of particle-to-fluid heat transfer in packed beds, Chem. Eng. Sci. 62 (2007) 6897–6907.
[16] A. Guardo et al., CFD study on particle-to-fluid heat transfer in fixed bed reactors: convective heat transfer at lowand high pressure, Chem. Eng. Sci. 61 (2007) 4341–4353.
[17] F. Kuwahara, T. Yamane, A. Nakayama, Large eddy simulation of turbulent flow in porous media, Int. Commun. Heat and Mass Transfer 33 (4) (2006) 411–418.
[18] F. Kuwahara, M. Shirota, A. Nakayama, A numerical study of interfacial convective heat transfer coefficient in two-energy equation model for convection in porous media, Int. J. Heat Mass Transfer 44 (6) (2001) 1153–1159.
[19] I. Ghosh, Heat-transfer analysis of high porosity open-cell metal foam, J. Heat Transfer 130 (2008) 034501.
[20] J. Petrasch et al., Tomography based determination of permeability, Dupuit–Forchheimer coefficient, and interfacial heat transfer coefficient in reticulate porous ceramics, Int. J. Heat and Fluid Flow 29 (1) (2008) 315–326.
[21] J. Petrasch et al., Tomography-based determination of the effective thermal conductivity of fluid-saturated reticulate porous ceramics, J. Heat Transfer 130 (2008) 032602.
[22] P.X. Jiang et al., Experimental and numerical investigation of forced convection heat transfer of air in non-sintered porous media, Exp. Therm. Fluid Sci. 28 (6) (2004) 545–555.
[23] J. Asme et al., Measurement of interstitial convective heat transfer and frictional drag for flow across metal foams, J. Heat Transfer 124 (2002) 120.

[24] K. Torii, K.M. Kwak, K. Nishino, Heat transfer enhancement accompanying pressure-loss reduction with winglet-type vortex generators for fin-tube heat exchangers, Int. J. Heat Mass Transfer 45 (18) (2002) 3795–3801.
[25] L.B. Younis, R. Viskanta, Experimental determination of the volumetric heat transfer coefficient between stream of air and ceramic foam, Int. J. Heat Mass Transfer 36 (6) (1993) 1425–1434.
[26] H.Y. Zhang, X.Y. Huang, Volumetric heat transfer coefficients in solid–fluid porous media: closure problem, thermal analysis and model improvement with fluid flow, Int. J. Heat Mass Transfer 43 (18) (2000) 3417–3432.
[27] H. Zhang, J. Tan, L. Zhang, Measurement of volumetric convective heat transfer coefficient in porous aluminum, J. Chem. Ind. Eng. 55 (010) (2004) 1710–1713.
[28] J.J. Hwang et al., Measurement of interstitial convective heat transfer and frictional drag for flow across metal foams, J. Heat Transfer 124 (2002) 120.
[29] Z. Wu et al., Numerical study of interfacial heat transfer between air flow and ceramic foams for optimizing volumetric solar air receiver, in: Proceedings of the International SolarPACES Symposium on Concentrating Solar Power and Chemical Energy Systems, Berlin, Germany, 2009.
[30] M.D. Montminy, A.R. Tannenbaum, C.W. Macosko, The 3D structure of real polymer foams, J. Colloid Interface Sci. 280 (1) (2004) 202–211.
[31] T.J. Lu, H.A. Stone, M.F. Ashby, Heat transfer in open-cell metal foams, Acta Mater. 46 (10) (1998) 3619–3635.
[32] M. Lacroix et al., Pressure drop measurements and modeling on SiC foams, Chem. Eng. Sci. 62 (12) (2007) 3259–3267.
[33] S. Krishnan, J.Y. Murthy, S.V. Garimella, Direct simulation of transport in open-cell metal foam, J. Heat Transfer 128 (2006) 793.
[34] K. Boomsma, D. Poulikakos, Y. Ventikos, Simulations of flow through open cell metal foams using an idealized periodic cell structure, Int. J. Heat Fluid Flow 24 (6) (2003) 825–834.
[35] K. Boomsma, D. Poulikakos, On the effective thermal conductivity of a three-dimensionally structured fluid-saturated metal foam, Int. J. Heat Mass Transfer 44 (2001) 827–836.
[36] J.T. Richardson, Y. Peng, D. Remue, Properties of ceramic foam catalyst supports: pressure drop, Appl. Catal. 204 (1) (2000) 19–32.
[37] J.C. Tannehill, D.A. Anderson, R.H. Pletcher, Computational Fluid Mechanics and Heat Transfer, Taylor & Francis Group, 1997.
[38] J. Ierardi, 2000. Available from: <http://users.wpi.edu/≃ierardi/firetools/air_prop.html>.
[39] M.J. Hall, J.P. Hiatt, Measurements of pore scale flowswithin and exiting ceramic foams, Exp. Fluids 20 (1996) 433–440.
[40] D.C. Wilcox, Turbulence modeling – An overview, AIAA 2001-0724, in: 39th Aerospace Sciences Meeting & Exhibit, Reno, Nevada, 2001.
[41] F.R. Menter, M. Kuntz, R. Langtry, Ten years of industrial experience with the SST turbulence model, Turbul. Heat Mass Transfer 4 (2003) 2003.
[42] W. Vieser, T. Esch, F. Menter, Heat transfer predictions using advanced two-equation turbulence models, CFX Validation Report, 2002.
[43] F.W. Dittus, L.M.K. Boelter, Heat transfer in automobile radiators of the tubular type, Int. Commun. Heat Mass Transfer 12 (1) (1985) 3–22.
[44] A.A. Zhukauskas, R. Ulinskas, Heat Transfer in Tube Banks in Crossflow, Taylor & Francis, 1988.
[45] N. Wakao, S. Kaguei, Heat and Mass Transfer in Packed Beds, Gordon and Beach, New York, 1982.
[46] B.P. Boudreau, The diffusive tortuosity of fine-grained unlithified sediments, Geochim. Cosmochim. Acta 60 (1996) 3139–3142.
[47] T.B. Boving, P. Grathwohl, Tracer diffusion coefficients in sedimentary rocks: correlation to porosity and hydraulic conductivity, J. Contam. Hydrol. (53) (2001) 85–100.
[48] P.F. Low, Principles of ion diffusion in clays, in: Chemistry in the Soil Environment, American Society for Agronomy, Special Publication, vol. 40, 1981, pp. 31–45.
[49] L. Shen, Z. Chen, Critical review of the impact of tortuosity on diffusion, Chem. Eng. Sci. 62 (14) (2007) 3748–3755.
[50] W.S. Janna, Engineering Heat Transfer, CRC Press, 2000.